Available online at www.sciencedirect.com
SCIENCE DIRECT®
ELSEVIER
Earth and Planetary Science Letters 220 (2004) 107–119
EPSL
www.elsevier.com/locate/epsl

Effects of thermo-chemical mantle convection on the thermal evolution of the Earth's core

Takashi Nakagawa [a,*], Paul J. Tackley [a,b]

[a] Department of Earth and Space Sciences, University of California, Los Angeles, CA 90095-1567, USA
[b] Institute of Geophysics and Planetary Physics, University of California, Los Angeles CA, 90095-1567, USA

Received 12 September 2003; received in revised form 18 December 2003; accepted 7 January 2004

Abstract

A coupled core-mantle evolution model that combines a global heat balance in the core with a fully dynamic thermo-chemical mantle convection model is developed to investigate the thermal evolution of the core over the 4.5 Gyr of Earth history. The heat balance in the core includes gravitational energy release, latent heat release and compositional convection associated with inner core growth. In the mantle convection model, compositional variations, plate-like behavior, phase changes and melting-induced differentiation are included. For mantle compositional variations, three idealized situations are considered: no variations (isochemical), variations resulting from a layered initial condition, and variations resulting from melting-induced differentiation from a homogeneous start. Only models whose thermal evolution satisfies three criteria are judged to be 'successful', with the criteria based on: (1) the radius of the inner core, (2) the heat flux through the core-mantle boundary (CMB), and (3) the heat flux through the surface. The radius of the inner core is the strictest criterion of these three. Models with an isochemical mantle fail because the inner core becomes much larger than the current size of the inner core. The final inner core radius is quite sensitive to mantle chemical buoyancy ratio. Models that fully satisfy all three criteria have a 1.5–2% compositional density difference, and either initial layering or compositional layering generated from melt-induced differentiation. These results imply that the heat flux buffering effect of a compositionally-dense layer in the deep mantle may be required to explain the thermal evolution of the core, when the heat flux through the CMB is calculated using a fully dynamical mantle convection model. Considering geochemical constraints, the compositional layering could be generated a combination of melt-induced differentiation and primordial layering. However, while the observed trends are robust, the models include various approximations and uncertainties, with the core model not including the effects of heat generated by radioactive element, so further investigations are warranted.

Keywords: thermal evolution; core-mantle boundary; mantle convection; inner core growth; compositional anomalies

1. Introduction

The strongly heterogeneous signature of the core-mantle boundary (CMB) region has been investigated in various seismological, geochemical and mantle convection modeling studies (e.g. [1–

* Corresponding author. Present address: Department of Geophysical Sciences, University of Chicago, Chicago, IL 60637, USA. Tel.: +1-310-825-9296; Fax: +1-310-825-2779.
E-mail address: takashi@ess.ucla.edu (T. Nakagawa).

0012-821X/04/$ – see front matter © 2004 Elsevier B.V. All rights reserved.
doi:10.1016/S0012-821X(04)00055-X

7]). It is commonly believed that this strong heterogeneity may be due, at least in part, to compositional anomalies above the CMB, the lateral variation of which may be an undulating layer, or isolated 'piles' of dense material [6–8]. A stable layer above the CMB may also provide an explanation for some geochemical constraints [5,9,10]. The two most common proposed origins of this anomalous material are: (1) primordial, i.e. the residue of the initial differentiation between the mantle and core (e.g. [11]), and (2) recycled, probably mainly oceanic crust that becomes segregated from subducted slabs [9,12]. A dense layer above the CMB would act as a strong buffer for the heat flux through the CMB, which, according to [13], may be parameterized in a similar manner to surface heat flux in a stagnant lid convection system, because the viscosity in a dense layer should be much lower than that in the lower mantle above it.

In previous modeling of the thermal evolution of the mantle and core, simple, parameterized mantle convection models [14–16] have been used to calculate the heat flux across the CMB, and coupled to a simple core heat balance that includes compositional convection and inner core growth [17–21]. Parameterized convection modeling is, however, not suitable for a system that includes laterally-varying (e.g. undulating or discontinuous) compositional anomalies above the CMB because it assumes a perfectly flat layer [22]. In addition to compositional variations, there are several other complexities in mantle convection, including phase changes and plate tectonics, that may be poorly represented in a parameterized model. Even the effect of strong viscosity variations on CMB heat transport is not known. Therefore, for understanding the thermal evolution of the Earth, it is important to use a fully dynamic mantle convection model combined with a parameterized core heat balance. The first example of such a fully-dynamical approach [23] simulated mantle convection with core-cooling, however, their models did not include chemical variations and did not explicitly discuss the thermal evolution of the Earth's core including inner core growth. Another study developed such a model based on thermo-chemical mantle convection [24] but the target of that study was to investigate the thermal and magnetic evolution of the Moon, not Earth.

Thus, the purposes of this study are: (1) to construct a coupled mantle–core model by combining a fully dynamical, thermo-chemical mantle convection model with a simple heat balance in the core, and use it to calculate thermal evolution histories for different assumptions about compositional heterogeneity, (2) to constrain acceptable scenarios by applying three criteria that a successful model must match (detailed later; based on the heat flux through the CMB, surface heat flux and the radius of the inner core), and thus (3) to determine whether mantle compositional layering is necessary to explain core thermal evolution, and if so, to constrain whether the origin of compositional anomalies above the CMB is more likely to be primordial or through differentiation.

Clearly, there are many uncertainties in both the mantle and core models, including uncertain parameter choices and various approximations that make the models not fully 'realistic' of the real Earth. The goal here is not an exhaustive mapping of parameter space, but rather, an exploratory investigation, in which the effect of different idealized assumptions about compositional heterogeneity is tested on a model that is otherwise unchanged between cases. The trends in behavior are expected to be robust, but the exact numbers may undergo refinement in future studies.

2. Model

2.1. Numerical model of mantle convection

The compressible anelastic and infinite Prandtl number approximations are assumed in a 2-D cylindrical shell with a ratio of inner to outer radii that is set such that the ratio of CMB surface area to outer surface area is the same as that in the real, spherical Earth. This radius rescaling was found by [25] to give essentially the same heat fluxes as in a spherical shell. The viscosity is temperature-, depth-, and yield stress-dependent, as

given below, and composition-independent phase changes are assumed at depths of 400 km (exothermic; Clapeyron slope +2.8 MPa/K) and 660 km (endothermic; −2.8 MPa/K). Depth-dependent density, thermal expansivity and thermal diffusivity are as in fig. 1 and table 1 of [8]. The internal heating rate R_h decreases with time and is enhanced by a factor of 10 in the dense material, i.e. $R_h(C,t) = H_0(1+9C)\exp((t_a-t)\ln 2/\tau)$ where τ is an averaged half life of radioactive elements, H_0 is the present-day heating rate in the regular mantle, t_a is the age of the Earth (4.5 Gyr) and t is the time since the beginning of the calculation. The averaged present-day internal heating rate in the mantle is set to be non-dimensional 23.7 (dimensionally 6.2×10^{-12} W/kg). Details of the model, numerical procedure and mathematical formulation have been given elsewhere [8,11,26–28]; thus, only summarized descriptions are given here. Composition is treated using two types of tracer particles, as in [29]. Chemical differentiation due to melting is also included in some cases, which is done by comparing, after each timestep, the local temperature to a depth-dependent solidus (shown in Fig. 1). When the temperature exceeds the solidus in a cell, the fraction of melt necessary to bring the temperature back to the solidus is generated and instantaneously placed at the surface to form crust, and the temperature is set back to the solidus [9] [28]. The physical parameters assumed in the mantle convection

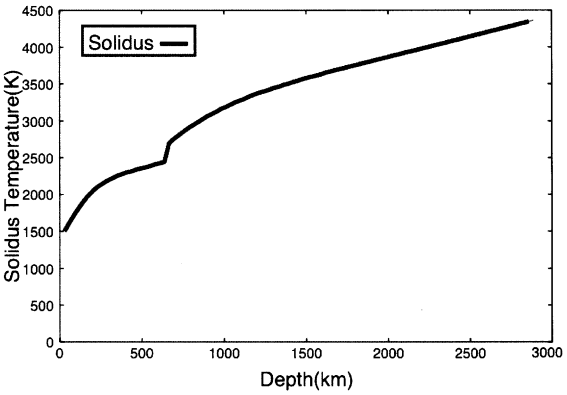

Fig. 1. Assumed depth-profile of mantle solidus temperature.

model are listed in Table 1. The viscosity law is as follows:

$$\eta_d(T,z) = \eta_0[1+(\Delta\eta-1)H(z-0.223)]\exp[4.6z]\exp\left[\frac{27.631}{T+1-T_s}\right]$$
$$\sigma_Y(z) = \sigma_b + \sigma_d z$$
$$\eta(T,z,\dot{e}) = \min\left(\eta_d(T,z), \frac{\sigma_Y(z)}{2\dot{e}}\right) \quad (1)$$

where $\eta_d(T,z)$ is the ductile viscosity, $\Delta\eta$ is the viscosity jump between upper and lower mantles, H is the Heaviside step function, $\sigma_Y(z)$ is the depth-dependent yield stress, σ_d is the yield stress gradient, σ_b is the yield stress at the surface, $\bar{e}$ is the second invariant of the strain rate tensor, T_s is

Table 1
Mantle model physical mantle parameters

Symbol	Meaning	Non-D. value	Dimensional value
Ra_0	Rayleigh number	10^7	N/A
η_0	Reference viscosity	1	1.4×10^{22}
$\Delta\eta$	Viscosity jump at 660 km	30	N/A
σ_b	Yield stress at surface	1×10^5	117 MPa
σ_d	Yield stress gradient	4×10^5	162.4 Pa m^{-1}
ρ_0	Reference (surface) density	1	3300 kg m^{-3}
g	Gravity	1	9.8 m s^{-2}
α_0	Ref. (surface) thermal expan.	1	5×10^{-5} K^{-1}
κ_0	Ref. (surface) thermal diff.	1	7×10^{-7} m^2 s^{-1}
ΔT_{sa}	Temperature scale	1	2500 K
T_s	Surface temperature	0.12	300 K
L_m	Latent heat	0.2	6.25×10^5 J kg^{-1}
τ	Half life	0.00642	2.43 Gyr

$Ra_0 = \rho_0 g\alpha_0\Delta T_{sa} d^3/\kappa_0\eta_0$.

the surface temperature and z is the vertical coordinate, which varies from 1 at the CMB to 0 at the surface. In this formulation, the viscosity changes by six orders of magnitude with temperature, two orders of magnitude with depth (though the increase along an adiabat is less), and $\Delta\eta$ across the 660 km discontinuity.

2.2. Thermal evolution of the core

The mathematical formulation of core thermal evolution is based on simple analytical models [17,30], which are composed of the equation of heat balance, latent heat release and gravitational energy release caused by the inner core growth:

$$\frac{4}{3}\pi(r_{CMB}^3-r_{IC}^3)\rho_c c_c \xi\frac{dT_{CMB}}{dt} = -4\pi r_{CMB}^2 F_{CMB} + 4\pi r_{IC}^2(E_G+L)\frac{dr_{IC}}{dt}$$

$$E_G = \Delta\rho_{IC} g r_{CMB}\left[\frac{3}{10}-\frac{1}{2}\left(\frac{r_{IC}}{r_{CMB}}\right)^2\right]$$

$$L = \rho_c T_L(r_{IC}, C_l)\Delta S \qquad (2)$$

where T_{CMB} is the temperature at CMB, r_{IC} is the radius of the inner core, E_G and L are gravitational energy and latent heat release, respectively, ξ is a constant for expressing adiabatic effect in the core and F_{CMB} is the heat flux through the CMB. Definitions of other variables and values of physical parameters are shown in Table 2. The onset of inner core growth is determined by using the relationship between the solidus of core-alloy and the adiabatic temperature profile calculated from the temperature at CMB. The growth rate of inner core is calculated from the heat balance equation. In order to express the compositional convection in the core caused by the separation between light elements and pure iron during the inner core growth, the density of core-alloy is calculated as:

$$\rho_c = \left[\frac{(1-C_l)}{\rho_{\mathrm{iron}}}+\frac{C_l}{\rho_{\mathrm{li}}}\right]^{-1} \qquad (3)$$

where ρ_{iron} is the density of pure iron, ρ_{li} is the density of light elements and C_l is the concentration of light elements in the core-alloy. The density of light elements is determined by using experimental data of density of pure iron (12 700 kg m^{-3} [31]) and initial density of core-alloy (12 300 kg m^{-3}). The concentration of light elements in the outer core is calculated based on the radius of the inner core by:

$$C_l = C_l(t=0)\left(\frac{r_{CMB}^3}{r_{CMB}^3-r_{IC}^3}\right). \qquad (4)$$

3. Experimental procedure

3.1. Resolution, boundary condition and initial condition

For the mantle convection model, a numerical grid of 256 (horizontal) × 64 (vertical) cells is used, with an average of 16 tracers per grid cell to track the composition. Side boundaries are periodic. Temperature is isothermal at top and bottom boundaries, with the CMB temperature de-

Table 2
Physical parameters for heat balance in the core

Symbols	Meanings	Values (units)
r_{CMB}	Radius of the core	3486 km
ρ_c	Init. density of core	12 300 kg m^{-3}
ρ_{iron}	Density of pure iron	12 700 kg m^{-3}
ρ_{li}	Density of light elements	4950 kg m^{-3}
$\Delta\rho_{IC}$	Density difference	400 kg m^{-3}
ΔS	Entropy change	118 J kg^{-1} K^{-1}
$C_l(t=0)$	Init. cont. of light elements	0.035
C_c	Heat capacity of the core	800 J kg^{-1} K^{-1}
$T_L(r=0,\ C_l(t=0))$	Melting T. at the center	5120 K

The value of entropy change is taken from [39]. All other values are taken from [16].

termined by using Eq. 2 with an initial value of 4300 K. This temperature is based on the solidus temperature at CMB (see Fig. 1). The velocity boundary conditions are impermeable and shear stress free at both horizontal boundaries. For chemical composition, a no vertical mass flux condition is implied at top and bottom boundaries. The initial condition for the temperature field is an adiabat with potential temperature 1925 K plus error function boundary layers at top and bottom plus small random perturbations. The initial condition for composition is either (1) layered, with a dense layer ($C=1$) of non-dimensional thickness 0.1 above the CMB and $C=0$ above it, or (2) homogeneous, with $C=0.3$. In the latter case, the end members $C=0$ and $C=1$ later evolve through melting.

3.2. Cases

Eight cases are considered: four with a compositionally-layered start and no subsequent differentiation, and four with a homogeneous start plus melting-induced chemical differentiation. The key parameter in each thermo-chemical scenario is the compositional buoyancy ratio:

$$B=\frac{\Delta\rho_c}{\rho_0\alpha_0\Delta T_{sa}} \tag{5}$$

where $\Delta\rho_c$ is the density difference caused by compositional variation, ρ_0 is the reference (surface) density, α_0 is the reference (surface) thermal expansivity, and ΔT_{sa} is the superadiabatic temperature scale. Four values of B are used here; 0, 0.12, 0.18 and 0.24, which correspond to density differences of up to 99 kg/m^3, which is 3% of the surface density ($\sim$1.8% of the density at the CMB). For the upper mantle and top of the lower mantle, this is low compared to mineral physical constratints [32], but it may be reasonable in the deep mantle where it is the most important. The case with $B=0$ and a layered start is effectively an isochemical case, since composition is purely passive. With differentiation included, the temperature is affected by latent heat absorption due to melting, so even with passive composition (i.e. $B=0$) the solution diverges from a purely isochemical case. Note that as in [6,8], B is based on surface parameters, and as thermal expansivity decreases with depth, stable layering is possible even with B much less than 1.

3.3. Criteria for a successful evolution

For a case to be judged 'successful', in the sense of being a plausible though non-unique representation of Earth's thermal evolution, it must satisfy three criteria: (1) the present-day surface heat flow must be consistent with the observational value ($\sim$38 TW or 76 mW/m^2 [33]), (2) the heat flux through the CMB must be consistent with the minimum heat flux (2 TW for the inner core radius = 1220 km to 10 TW if no inner core) to maintain the magnetic field through geodynamo action [17,21,34], for at least the last 3 billion years, and (3) the present-day radius of the inner core must be consistent with seismological measurements ($\sim$1220 km) [35]. Note that the total heat flow values (in TW) that are later quoted for various cases are calculated from model heat flux values by assuming a spherical core of the actual radius, consistent with the finding of [25] that a rescaled-radius cylindrical model gives the same heat flux as an actual-radius spherical model.

4. Results

4.1. Isochemical and B = 0 differentiating cases

Fig. 2 shows the time variation of heat flux through the CMB and surface, temperature at the CMB and inner core radius for cases in which composition is passive ($B=0$), which, for the non-differentiating case, is equivalent to isochemical. The thermal evolution is similar for both cases and fails because the radius of the inner core exceeds the present-day value ($\sim$1220 km), growing to approximately 2200 km. At the present time the temperature at the CMB in both cases is around 3300 K, the total heat flow through the CMB is around 70 mW/m^2 (equivalent to 11 TW), which is a reasonable value judging by the criteria, and the surface heat flux is around the present-day value. However, an isochemical man-

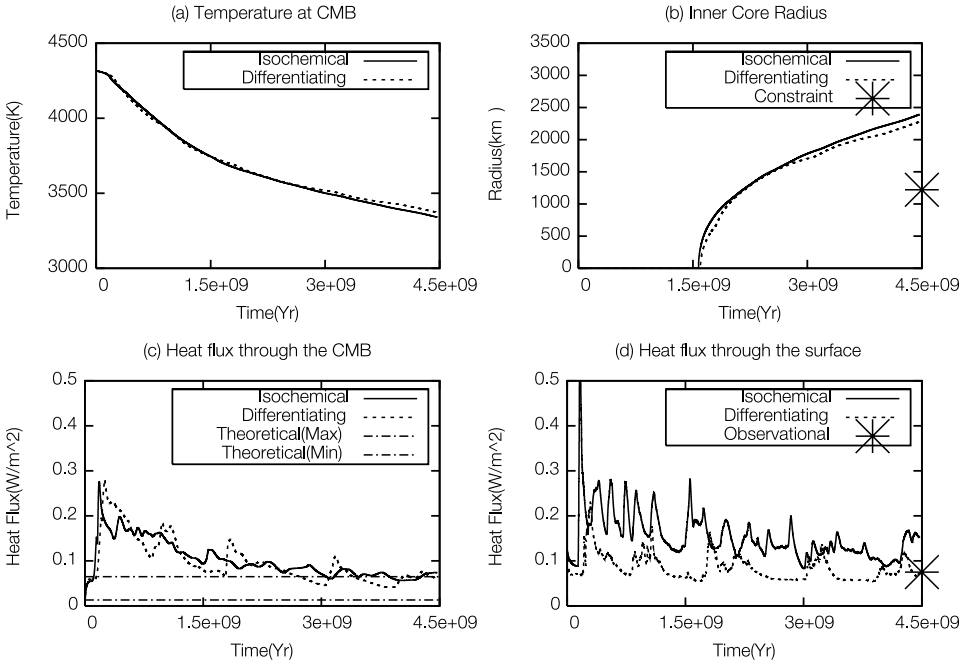

Fig. 2. Time evolution for passive-composition ($B=0$) cases (isochemical and differentiating). (a) Temperature at CMB. (b) Radius of the inner core. (c) Heat flux through the CMB. (d) Heat flux through the surface. The dotted line in (c) shows the heat flux required to maintain the magnetic field by geodynamo action. The large asterisk symbol in (b) and (d) shows the present-day inner core radius and heat flux obtained from observational data, respectively.

tle, at least with the parameters assumed here, appears inconsistent with the constraint for the radius of the inner core on Earth's thermal evolution.

4.2. Layered start

Fig. 3 shows the time evolution of temperature at the CMB, heat fluxes through both boundaries and the radius of the inner core for the three cases with a layered start (no differentiation) and different buoyancy ratios. The cooling rate of the CMB during 4.5 Gyr varies from approximately 120 K/Gyr to 163 K/Gyr. This range is similar to that used by theoretical models of core thermal evolution constructed using the physical properties of the core [36,37]. The heat flux through the CMB is always similar to or higher than the estimated minimum heat flux required to maintain the geodynamo, implying that the magnetic field can be generated during the whole 4.5 Gyr of Earth history. The present-day inner core radius varies from 0 km ($B=0.24$) to 1500 km ($B=0.12$), while the present-day surface heat flux is only slightly higher than the observed value. A large spike at around 100 Myr from the start corresponds to the initiation of plate-like behavior. From these criteria, two cases ($B=0.12$ and $B=0.18$) are judged to be relatively reasonable evolution models.

Fig. 4 shows snapshots of the temperature and compositional fields for a 'successful' case ($B=0.12$; Fig. 4a) and the 'failed' case ($B=0.24$; Fig. 4b). With the lower buoyancy ratio (Fig. 4a), topography on the layer is so large that it is swept into hot, isolated piles by subducted slabs. Slabs are then able to reach exposed regions of the CMB, increasing the core heat flux and growth rate of the inner core. With denser material (Fig. 4b), undulations of the compositional boundary are formed by subducted slabs but the CMB is covered everywhere, reducing the CMB heat flux. Subducted slabs are often bent at the

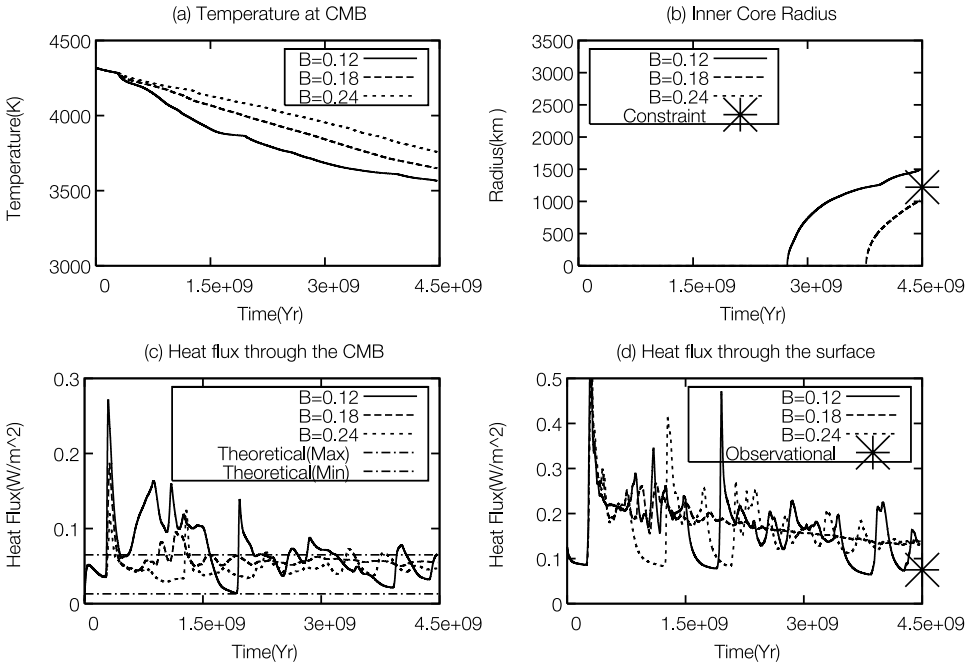

Fig. 3. Time evolution for the layered start cases. (a) Temperature at CMB. (b) Radius of the inner core. (c) Heat flux through the CMB. (d) Heat flux through the surface.

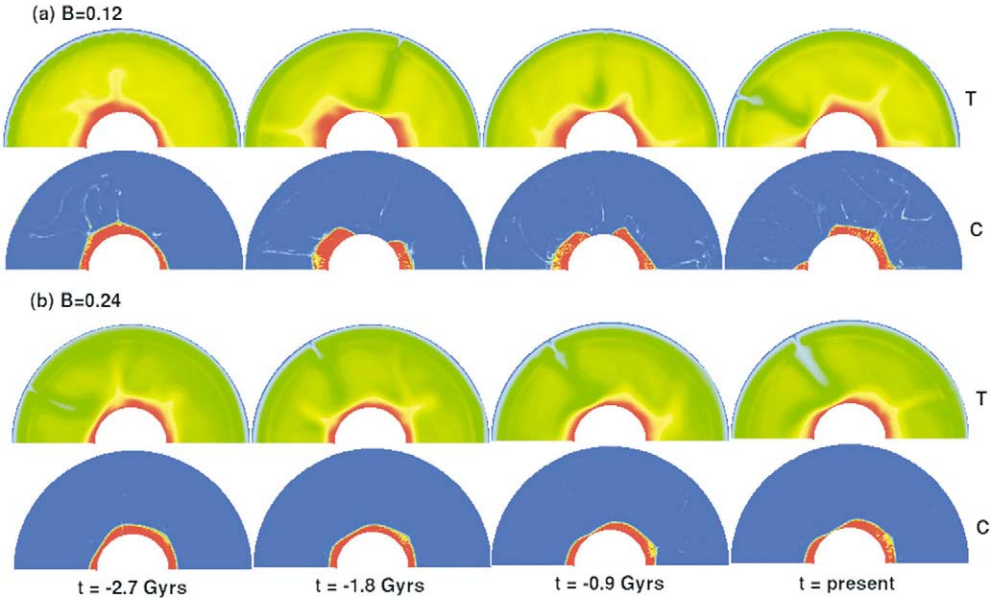

Fig. 4. Structural evolution for layered start cases. (a) $B = 0.12$. (b) $B = 0.24$. The top row in both (a) and (b) shows the temperature field and the bottom row shows the compositional field. Red: high temperature and composition. Blue: low temperature and composition.

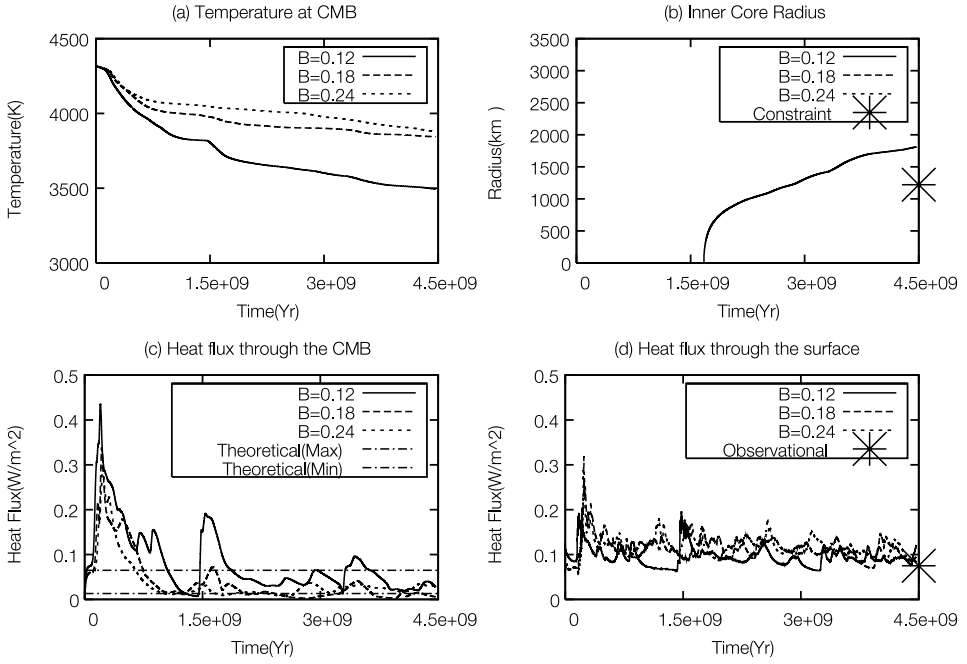

Fig. 5. Time evolution for differentiating, homogeneous start cases. (a) Temperature at CMB. (b) Radius of the inner core. (c) Heat flux through the CMB. (d) Heat flux through the surface.

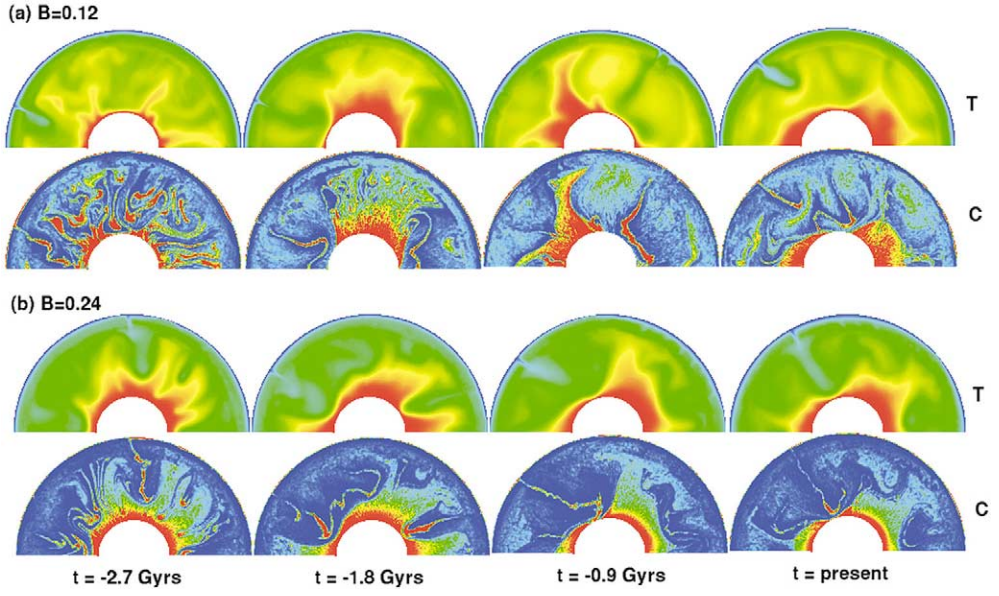

Fig. 6. Structural evolution for differentiating, homogeneous start cases. (a) $B = 0.12$. (b) $B = 0.24$. The top row in both (a) and (b) shows the temperature field and the bottom row shows the compositional field. Red: high temperature and composition. Blue: low temperature and composition.

660 km discontinuity because of the endothermic phase change and viscosity jump at that depth.

4.3. Differentiating from a homogeneous start

Fig. 5 shows the time variation of heat fluxes, CMB temperature and inner core radius for these cases. The lowest buoyancy ratio ($B = 0.12$) case is reasonably successful, but the radius of the inner core, which is around 1800 km, exceeds the constraint. With the intermediate buoyancy ratio ($B = 0.18$) and the highest buoyancy ratio ($B = 0.24$), there is no inner core at the present time. The most successful buoyancy ratio seems to be between $B = 0.12$ and $B = 0.18$ because the heat flux through the CMB is dependent on the buoyancy ratio. Interestingly, the surface conductive heat flux is almost constant with time after an early peak, at around the observed present-day value, which is probably due to the buffering effect of melting and melt-related heat transport on conductive heat flow. This jump and peak in surface heat flux at around 100 Myr corresponds to the onset of plate-like behavior.

Fig. 6 shows snapshots of temperature and compositional field for the lowest (Fig. 6a) and highest (Fig. 6b) buoyancy ratio cases. In both cases shown in Fig. 6, a dense layer forms above the CMB due to the accumulation of segregated crustal material from subducted slabs, as in previous studies [9,12]. In the lowest buoyancy ratio case (Fig. 6a), the dense layer forms very high isolated piles and subducted slabs can completely sweep the dense material into upwelling regions. The highest buoyancy ratio (Fig. 6b) results in a flatter and more stable layer but small height of isolated piles with small topography form above the CMB. Subducted slabs are bent at the 660 km discontinuity as in the layered start cases.

4.4. Comparison between the two idealized compositional end-members

The major difference between these two compositional scenarios is the time history of heat flux through the CMB, which is strongly related to the presence or absence of a dense layer above the CMB. With a layered start and sufficiently dense layer, the heat flux through the CMB stabilizes, after an early pulse, to the range of 60 mW/m^2 (equivalent to 10 TW), which is sufficient to maintain the geodynamo. With a homogeneous start, the CMB heat flux is very much larger until a dense layer has built up, which takes $\sim$1.5 Gyr. After a dense layer built up above the CMB region, the CMB heat flux stabilizes to the range from 30 mW/m^{-2} (5 TW) to 60 mW/m^{-2} as in cases with a layered start, which is also sufficient to maintain the geodynamo. Comparing the surface heat flux, melt-related heat transport, which may transport a significant fraction of the total heat particularly early in Earth's evolution, is not operating in the layered start cases. A successful evolution is found when the density difference of basaltic material is relatively low (1.5–2%). Therefore either origin of compositional anomalies in the CMB region is possible from the perspective of thermal evolution.

5. Discussion

5.1. Thermo-chemical structure in the convecting mantle

These results suggest that a compositionally-dense layer above the CMB is necessary to reduce the rate of core cooling sufficiently to prevent core freezing, while at the same time allowing sufficient heat flux to drive the geodynamo. From a comparison of the two end-member compositional assumptions, it appears that initial (or very early) layering with a density of 1.5–2% is necessary to prevent very high CMB flux and rapid core cooling early on. This density difference is consistent with an estimate from a seismic tomography-based mantle dynamics model [38]. For the thermal evolution of the Earth's core, both end-members are plausible, as judged by the heat flux through the CMB and size of the inner core, Considering geochemical constraints, segregation of recycled crust (eclogite) rather than initial layering the segregation of recycled crust (eclogite) at the CMB may well be necessary to explain the 'recycled' trace element isotopic signatures of MORB and OIB, as indicated, for example, by

numerical models of thermo-chemical convection that include melting-induced differentiation of both major and trace elements [9,12,28]. At the same time, noble gas isotope ratios indicate the existence of primitive material, possibly in the deep mantle. Thus, from geochemical constraints, compositional anomalies may be generated by a combination of initial layering and the segregation of recycled crust [7].

5.2. Heat flux and temperature in the CMB region

Several analytical models of core thermal evolution have attempted to constrain the heat flux through the CMB required for maintaining the magnetic field generated by the geodynamo [17,19,21,38]. The minimum heat flux through the CMB has been estimated to be between 2 TW (1220 km inner core radius) to 10 TW (no inner core) [34]. In our 'successful' cases, the heat flux through the CMB is around 4 TW at present time, which is sufficient for the magnetic field to be maintained by the geodynamo at that inner core size.

The present-day CMB temperature in our 'successful' models is around 3600 K, which, although within the range of historical CMB estimates (e.g. [40]), is somewhat lower than recent estimates obtained from mineral physics considerations of the core solidus, for example 3950–4200 K calculated by [41]. The mantle solidus at the CMB is likely to be 4300 K maximum [40]. Thus, present-day CMB temperatures that are much higher would involve substantial melting of the deep mantle in the past, and possibly at present. Some recent seismological studies of the CMB region have suggested the existence of partially-molten patches that are thin and localized [1] [43,44], which suggests that a higher CMB temperature is indeed plausible, but places limits on how high it can be. One recent parameterized core and mantle model that includes radioactive heat production in the core [45] obtains a present-day CMB temperature as high as 4500 K, which should cause pervasive deep mantle melting. In our model, which does not include radiogenic heat production in the core, increasing the initial CMB temperature would certainly lead to a higher present-day CMB temperature (but would lead to problems with deep mantle melting earlier on), but the very rapid cooling of the core obtained in isochemical cases (Fig. 2a) indicates that it would have to be excessively high to prevent total freezing of the core. A chemical layer above the CMB would still be necessary to prevent core freezing for any reasonable initial CMB temperature.

5.3. Radioactive heat sources in the core

In our coupled model, it is assumed that radioactive heat production in the core is negligible, as has generally been assumed. Whether radiogenic elements such as ^{40}K are significant in the core is controversial, but recent studies involving analytic models of core thermal evolution [21,34,38] or geochemical experiments [46,47] have suggested that radioactive heat sources (particularly ^{40}K) may play an important role in explaining heat flux through the CMB, with some estimates [21,46] putting the radiogenically-produced component at 20% of the total. However, geochemical constraints [46] indicate that the presence of sulfur is required for potassium to be present. If the light element in the core alloy is not sulfur, the effect of internal heating by ^{40}K will thus be negligible. For the purposes of the initial models in this paper, this latter assumption has been made.

5.4. Melting temperature of the core-alloy

To determining the onset of inner core growth, the melting temperature of pure iron is required. There are three types of melting temperature profile that have been proposed by several groups: (1) Boehler type [48,49], (2) Anderson and Duba type [50], and (3) Williams type [51,52]. The difference among these three profiles is the melting temperature at the center, for which the Boehler type (5200 K) is the lowest and the Willams type is the highest (8000 K), with the Anderson–Duba type being approximately 6500 K at the center. In our model, the Boehler type is used for the solidus of the core and for determining the onset of the inner core growth. When an Anderson–Duba or Williams type melting temperature is used, there

is huge inner core at the beginning of the calculation. Such a scenario, in which an initial inner core first shrinks then grows again, may be possible according to parameterized modeling that includes radiogenic heat production in the core [42], if the solidus is higher than the Boehler type. Using numerical modeling based on thermodynamics [53], the melting temperature at the ICB (inner core boundary) has been estimated to be around 6200 K, which is close to the Anderson–Duba type. The temperature difference between ICB and the center of the Earth is approximately 100 K. However, numerical modeling of the elastic properties of the inner core [53] found that the temperature at ICB may be 5600 K. The sensitivity of the radius of the inner core as a function of time to these uncertainties must be checked in future modeling.

5.5. *Shortcomings of the mantle convection model*

When compared to the real Earth, there are numerous shortcomings and parameter uncertainties in the mantle convection model that could affect the results. The largest of these may be rheology, which is much less temperature-dependent than in the real Earth (making the heat flux less sensitive to mantle temperature) and does not include the full material complexity (e.g. history-dependence) that is relevant to the lithosphere and plate tectonics. The reference viscosity (based on the reference adiabat in the shallow mantle) is higher than realistic by perhaps an order of magnitude [45,54], but in thermal evolution situations the viscosity and 'effective' Rayleigh number self-adjust to rid the mantle of the generated heat [55]. The temperature-dependence of other material properties, such as thermal conductivity, may also be important [56,57].

Various parameters are uncertain, including the initial mantle adiabat and details of initial layering. If the initial adiabat were much higher it would exceed the solidus [28] so massive deep mantle melting would be expected, which would be difficult to treat in the model.

The robustness of results to model approximations and parameter choices must certainly be tested in the future, but it seems likely that while quantitative results may change, the trends in behavior observed here will be robust.

6. Conclusions

A coupled core-mantle evolution model that combines an analytic heat balance model for the core with a fully dynamical thermo-chemical mantle convection model has been developed for studying the thermal evolution of the core. The conclusions from the initial modeling presented in this paper are: (1) the presence of a dense, compositionally-distinct layer above the CMB is required to produce acceptable thermal evolution histories by reducing core cooling and inner core growth, and the origin of such a dense layer might be a combination of primordial layering and melt-induced differentiation, which is the segregation of eclogitic material from the oceanic crust, (2) successful thermal evolution is obtained for cases with a 1.5–2% compositional density variation and either initial layering or layering generated from melt-induced differentiation and crustal segregation, which is consistent with a density estimate from mineral physics [32] or a seismic tomography-based dynamical model [38], (3) the heat flow through the CMB in successful cases is equivalent to around 5–10 TW through geological time, which is sufficient for maintaining the geodynamo.

In future these preliminary findings must be verified by using models that include more realistic physics and test the effect of parameter uncertainties. For the core, this includes radiogenic heat generation by ^{40}K [20,36] and estimates of the nominal magnetic field, while for the mantle, a more realistic (e.g. more temperature-dependent) rheology, and the robustness of results to various parameter choices (e.g. initial thickness of compositional layer, initial adiabat, phase diagram and temperature- or composition-dependent physical properties (see [56] and [57]), must be tested. Lateral variations of heat flow through the CMB and the formation of an ultra low velocity zone (ULVZ) in the CMB region (which might be assisted by intense viscous heating with-

in the dense material [58]) could also be studied in the future.

Acknowledgements

This study was financially supported by the David and Lucile Packard Foundation. We thank Stephane Labrosse for valuable comments and discussions, David Price for information about the melting temperature and physical properties in the core, and Dave Yuen, Bruce Buffett and an anonymous reviewer for helpful reviews that improved the manuscript.*[SK]*

References

[1] T. Lay, Q. Williams, E.J. Garnero, The core–mantle boundary layer and deep Earth dynamics, Nature 392 (1998) 461–468.
[2] M. Ishii, J. Tromp, Normal mode and free-air gravity constraints on lateral variations in velocity and density of Earth's mantle, Science 285 (1999) 1231–1235.
[3] G. Masters, G. Laske, H. Bolton, A. Dziewonski, The relative behavior of shear velocity, bulk sound speed, and compressional velocity in the mantle: Implications for chemical and thermal structure, in: S. Karato et al. (Eds.), Earth's Deep Interior: Mineral Physics and Seismic Tomography from Atomic to the Global Scale, Am. Geophys. Union, Washington, DC, 2000, pp. 63–87.
[4] A.W. Hofmann, Mantle geochemistry: The message from oceanic volcanism, Nature 385 (1997) 219–229.
[5] N. Coltice, Y. Ricard, Geochemical observation and one layer mantle convection, Earth Planet. Sci. Lett. 174 (1999) 125–137.
[6] P.J. Tackley, The strong heterogeneity caused by deep mantle layering. Geochem. Geophys. Geosyst. 3 (2002) 2001GC000167.
[7] T. Nakagawa, P.J. Tackley, Thermo-chemical structures in the mantle arising from a three-component convective system and implications for geochemistry. Phys. Earth. Planet. Int. (2003) accepted.
[8] P.J. Tackley, Three dimensional simulation of mantle convection with a thermo-chemical boundary layer: D″? In: M. Gurnis, M.E. Wysession, E. Knittle, B.A. Buffett (Eds.), Core–Mantle Boundary Region, Am. Geophys. Union, Washington, DC, 1998, pp. 231–253.
[9] U.R. Christensen, A.W. Hoffmann, Segregation of subducted oceanic crust in the convecting mantle, J. Geophys. Res. 99 (1994) 19867–19884.
[10] L.H. Kellogg, B.H. Hager, R.D. van der Hilst, Compositional stratification in the deep mantle, Science 283 (1999) 1881–1884.
[11] D.J. Stevenson, Fluid dynamics of core formation, in: H.E. Newsom, J.H. Jones (Eds.), Origin of the Earth, Oxford University Press, New York, 1990, pp. 231–249.
[12] P.J. Tackey, S. Xie, The thermochemical structure and evolution of Earth's mantle: Constraints and numerical models, Philos. Trans. R. Soc. Lond. A 360 (2002) 2593–2609.
[13] V.S. Solomatov, L.-N. Moresi, Small-scale convection in the D′ layer. J. Geophys. Res. 107 (2002) 10.1029/2000JB000063.
[14] D.J. Stevenson, T. Spohn, G. Schubert, Magnetism and thermal evolution of the terrestrial planets, Icarus 54 (1983) 466–489.
[15] D. Breuer, T. Spohn, Possible flush instability in mantle convection at the Archaean–Proterozoic transitions, Nature 378 (1995) 608–610.
[16] T. Yukutake, The inner core and surface heat flow as clues to estimating the initial temperature of the Earth's core, Phys. Earth Planet. Int. 121 (2000) 103–137.
[17] B.A. Buffett, H.E. Huppert, J.R. Lister, A.W. Woods, On the thermal evolution of the Earth's core, J. Geophys. Res. 101 (1996) 7989–8006.
[18] S. Labrosse, J.-P. Poirier, J.-L. Mouel, On cooling of the Earth's core, Phys. Earth Planet. Int. 99 (1997) 1–17.
[19] I. Sumita, S. Yoshida, Thermal interaction between the mantle, outer and inner cores, and the resulting structural evolution of the core, in: V. Dehant, K.C. Creager, S.-i. Karato, S. Zatman (Eds.), Earth's Core: Dynamics, Structure, Rotation, Am. Geophys. Union, Washington, DC, 2002, pp. 213–231.
[20] B.A. Buffett, Estimates of heat flow in the deep mantle based on the power requirements for the geodynamo. Geophys. Res. Lett. 29 (2002) 10.1029/2001GL014649.
[21] S. Labrosse, Thermal and magnetic evolution of the Earth's core. Phys. Earth Planet. Int. (2003) submitted.
[22] T. Nakagawa, P.J. Tackley, Effects of compositional heterogeneity on the thermal evolution of the convecting mantle and core, EOS Trans. AGU, 83 (2002) Fall Meet. Suppl., Abstract MR11A-10.
[23] V. Stenbach, D.A. Yuen, W. Zhao, Instabilities from phase transitions and the timescales of mantle thermal evolution, Geophys. Res. Lett. 20 (1993) 1119–11122.
[24] D.R. Stegman, A.M. Jellinek, S.A. Zatman, J.R. Baugardner, M.A. Richard, An early lunar core dynamo driven by thermo-chemical mantle convection, Nature 421 (2003) 143–146.
[25] P.E. Van Keken, Cylindrical scaling for dynamical cooling model of the Earth, Phys. Earth Planet. Int. 124 (2001) 119–130.
[26] P.J. Tackley, Self-consistent generation of tectonic plates in time-dependent, three-dimensional mantle convection simulations, part 1: pseudo-plastic yielding. Geochem. Geophys. Geosyst. 1 (2000a) 2000GC000036.
[27] P.J. Tackley, Self-consistent generation of tectonic plates in time-dependent, three-dimensional mantle convection simulations, part 2: Strain rate weakening and atheno-

sphere. Geochem. Geophys. Geosyst. 1 (2000b) 2000GC-000043.
[28] S. Xie, P.J. Tackley, Evolution of helium and argon isotopes in a convecting mantle. Phys. Earth Planet. Int. (2003) submitted.
[29] P.J. Tackley, S.D. King, Testing the tracer ratio method for modeling active compositional fields in mantle convection simulations. Geochem. Geophys. Geosyst. 4 (2002) 2001GC000214.
[30] B.A. Buffett, H.E. Huppert, J.R. Lister, A.W. Woods, Analytical model for solidification of the Earth's core, Nature 356 (1992) 329–331.
[31] D.M. Sherman, The composition of the Earth's core: Constraints on S and Si vs. temperature, Earth Planet. Sci. Lett. 153 (1997) 149–155.
[32] S. Ono, E. Ito, T. Katsura, Mineralogy of subducted basaltic crust (MORB) from 25 to 37 GPa, and chemical heterogeneity of the lower mantle, Earth Planet. Sci. Lett. 190 (2001) 57–63.
[33] H.N. Pollack, S.J. Hunter, R. Johnston, Heat loss from the Earth's interior: Analysis of the global data set, Rev. Geophys. 31 (1993) 267–280.
[34] B.A. Buffett, The thermal state of Earth's core, Science 299 (2003) 1675–1677.
[35] A.M. Dziewonski, D.L. Anderson, Preliminary reference Earth Model, Phys. Earth Planet. Int. 25 (1981) 297–356.
[36] D. Gubbins, D. Alfe, G. Masters, D. Price, M.J. Gillan, Can the Earth's dynamos run on heat alone? Geophys. J. Int. (2003) in press.
[37] D. Gubbins, D. Alfe, G. Masters, D. Price, M.J. Gillan, Gross thermodynamics of 2-component core convection. Geophys. J. Int. (2003) in press.
[38] A.M. Forte, J.X. Mitrovica, Deep-mantle high viscosity flow and thermochemical structure inferred from seismic and geodynamics data, Nature 410 (2001) 1049–1056.
[39] S. Labrosse, J.-P. Poirier, J.-L. Mouel, The age of the inner core, Earth Planet. Sci. Lett. 190 (2001) 111–123.
[40] F.D. Stacey, Physics of the Earth, 3rd ed., Brookfield Press, Australia, 1992, 513 pp.
[41] G.D. Price, D. Alfe, L. Vocadlo, M.J. Gillan, The Earth's Core: An Approach from First Principles, 2003, in preparation.
[42] A. Zerr, A. Diegeler, R. Boehler, Solidus of Earth's Deep Mantle. Nature (1998) 243–246.
[43] J.E. Vidale, M.A.H. Hedlin, Evidence for a partial melting at the core–mantle boundary north of Tonga from the strong scattering of seismic wave. Nature (1998) 682–685.
[44] Q. Williams, E.J. Garnero, Seismic evidence for partial melt at the base of Earth's mantle, Science 273 (1996) 1528–1530.
[45] F. Nimmo, G.D. Price, J. Brodholt, D. Gubbins, The influence of potassium on core and geodynamo evolution, Geophys. J. Int. (2003) submitted.
[46] C.L. Gessmann, B.J. Wood, Potassium in the Earth's core, Earth Planet. Sci. Lett. 200 (2002) 63–78.
[47] V. Rama Murthy, W. van Westrenen, Y. Fei, Radioactive heat source in planetary cores: Experimental evidence for potassium, Nature 423 (2003) 164–165.
[48] R. Boehler, Temperature in the Earth's core from melting point measurements of iron at high static pressures, Nature 363 (1993) 534–536.
[49] R. Boehler, High-pressure experiments and the phase diagram of lower mantle and core material, Rev. Geophys. 38 (2000) 221–245.
[50] O.L. Anderson, A. Duba, Experimental melting curve of iron revisited, J. Geophys. Res. 102 (1997) 22659–22669.
[51] Q. Williams, R. Jeanloz, J. Bass, R. Svenson, T.J. Ahrens, The melting curve of iron to 250 Gigapascals: A constraint on the temperature at Earth's center, Science 236 (1987) 181–182.
[52] Q. Williams, E. Knittle, R. Jeanloz, The high-pressure melting curve of iron: A technical discussion, J. Geophys. Res. 96 (1991) 2171–2184.
[53] D. Alfe, M.J. Gillan, D.G. Price, Composition and temperature of the Earth's core constrained by ab initio calculations and seismic data, Earth Planet. Sci. Lett. 195 (2002) 91–98.
[54] S.L. Butler, W.R. Peltier, Thermal evolution of Earth: Models with time-dependent layering of mantle convection which satisfy the Urey ratio constraint, J. Geophys. Res. 107 (2002) 10.1029/2000JB000018.
[55] D.C. Tozer, The present thermal state of the terrestrial planets, Phys. Earth Planet. Int. 6 (1972) 182–197.
[56] M. Manga, R. Jeanloz, Implications of metal-bearing chemical boundary layer in D″ for mantle dynamics, Geophys. Res. Lett. (1996) 3091–3094.
[57] F. Dubuffet, D.A. Yuen, E.S.G. Rainey, Control thermal chaos in the mantle by possible feedback from radiative thermal conductivity, Nonlin. Proc. Geophys. 9 (2002) 311–323.
[58] U. Hansen, D.A. Yuen, Extended Boussinesq thermal–chemical convection with moving heat source and variable viscosity, Earth Planet. Sci. Lett. 176 (2000) 401–411.